P.G. Coelho[1]*, E.A. Bonfante[1],
N.R.F. Silva[1], E.D. Rekow[2],
and V.P. Thompson[1]

[1]Department of Biomaterials and Biomimetics and [2]Department of Basic Science and Craniofacial Biology, New York University College of Dentistry, 345 24th St. 804s, New York, NY 10010, USA ; *corresponding author, pgcoelho@nyu.edu

# Laboratory Simulation of Y-TZP All-ceramic Crown Clinical Failures

## ABSTRACT

Clinically, zirconia-supported all-ceramic restorations are failing by veneer-chipping without exposing the zirconia interface. We hypothesized that mouth motion step-stress-accelerated fatigue testing of standardized dental crowns would permit this previously unrecognized failure mode to be investigated. Using CAD software, we imported the average dimensions of a mandibular first molar crown and modeled tooth preparation. The CAD-based tooth preparation was rapid-prototyped as a die for fabrication of zirconia core porcelain-veneered crowns. Crowns were bonded to aged composite reproductions of the preparation and aged 14 days in water. Crowns were single-cycle-loaded to failure or mouth-motion step-stress-fatigue-tested. Finite element analysis indicated high stress levels below the load and at margins, in agreement with only single-cycle fracture origins. As hypothesized, the mouth motion sliding contact fatigue resulted in veneer chipping, reproducing clinical findings allowing for investigations into the underlying causes of such failures.

**KEY WORDS:** single-crown, all-ceramic, mechanical testing, step-stress fatigue, finite element analysis.

## INTRODUCTION

Despite the biocompatibility and esthetic appeal of all-ceramic crowns, fracture of the veneer or the core remains the major clinical reason for technical complications in the posterior region (Pjetursson *et al.*, 2007). Mouth motion fatigue of crown-like structures causes failure, initiating from the point of load application in the form of outer and inner cone cracks, which propagate to the veneer/core interface (Rekow and Thompson, 2007). Restorations may also fail when the cementation surface of the core material is subjected to repeated tensile stresses near its bulk flexure strength, resulting in radial crack failure (Kelly, 1999; Bhowmick *et al.*, 2007b; B Kim *et al.*, 2007). Currently, no laboratory test method simulates the clinical failures observed.

Great effort has been expended in the development of more reliable ceramics. Fracture strengths have been progressively increased from glass-ceramic (Empress II, 320 MPa) to alumina (547 MPa) to zirconia (900 MPa) (Deng *et al.*, 2002). The high value found for the latter, similar to that of metals such as steel (Manicone *et al.*, 2007), has encouraged its use for hip and knee replacements and dental crowns, fixed partial dentures (FPD), and implants (Kohal and Klaus, 2004; Kohal *et al.*, 2006). The intermediate elastic modulus of zirconia is an advantage in reinforced layered structures, shifting damage and fracture modes into the porcelain veneer layer (Kim *et al.*, 2007a). Only recently reported is a fatigue study on anatomically correct crowns which reported cohesive failure in the porcelain veneer and in the veneer/core bond (Zahran *et al.*, 2008). This study used uni-axial loading, where the tooth-cusp-simulating indenter did not lift off the porcelain. In mouth-motion-like fatigue (indenter contact-load-slide-liftoff) of crown-like layered specimens, partial cone cracks develop beneath the sliding path at greater depth and steeper angle than uni-axial loading cone cracks. Also, these more aggressive cone cracks quickly propagate to the interface, resulting in the loss of veneer material (B Kim *et al.*, 2007).

Limited clinical data are available concerning the reliability of zirconia core-porcelain veneer crowns. A recent *in vitro* investigation found that the most common failure mode of either heat-pressed or sintered zirconia crowns was cohesive in the porcelain veneer layer (not directly observed during fatigue, but with load to failure testing following fatigue) (Tsalouchou *et al.*, 2008). Zirconia framework damage has not been reported in three-unit posterior fixed partial denture clinical studies. However, porcelain veneer cohesive failures have led to concerns regarding differences in coefficient of thermal expansion between the core and veneering porcelain and their respective processing techniques (Raigrodski *et al.*, 2006). One five-year clinical study of three- to five-unit zirconia framework fixed partial dentures found 15.2% failures from chipping of the porcelain veneer layer, but no framework failures

(Sailer *et al.*, 2007). While zirconia provides strength, clinical failure modes suggest that future development should focus on porcelain veneer materials.

This study was designed to evaluate an all-ceramic crown fatigue test method that would reproduce clinical failure modes. We applied mouth-motion fatigue loading to assess the reliability of anatomically correct all-ceramic zirconia single crowns cemented onto a standardized mandibular molar model. We hypothesized that mouth motion step-stress-accelerated fatigue testing of standardized dental crowns would allow this previously unrecognized failure mode to be investigated.

## MATERIALS & METHODS

### Computer Modeling

An anatomically correct 3-D CAD model of a mandibular first molar posterior tooth full-crown preparation and bilayer all-ceramic crown was generated. The solid components of the crown system consisted of a veneer layer (porcelain), a core layer (zirconia) of uniform thickness (0.5 mm), a 100-μm-thick cement layer (resin cement), and a tooth preparation (dentin) created in CAD software (Pro/Engineer Wildfire, PTC, Needham, MA, USA) (Figs. 1a, 1b). The components were assembled (Fig. 1c), imported into FEA software (Pro/Mechanica, PTC, Needham, MA, USA), meshed (~ 16,000 tetrahedral elements), and tested for convergence prior to mechanical simulation.

The FEA model assumptions were that: (1) all solids were homogeneous, isotropic, and linear elastic; (2) there were no slip conditions (perfect bonding) among components; (3) there was a uniform cement layer (elastic modulus, E = 8 GPa, and Poisson's ratio, $v = 0.33$); (4) there was a 0.5-mm zirconia core thickness (E = 205 GPa, $v = 0.19$); (5) there was a five-cusp porcelain veneer layer (E = 70 GPa, $v = 0.19$) 1 mm thick on the axial walls and 1.5 mm thick on the occlusal surface; (6) there was a dentin tooth core (E = 16 GPa, $v = 0.33$); (7) there were no flaws in any components; and (8) there was a six-degrees-of-freedom (full) constraint on the root component surface. Loads were applied over a 1-mm-diameter circle, simulating a typical occlusal contact area, at the mesial-distal
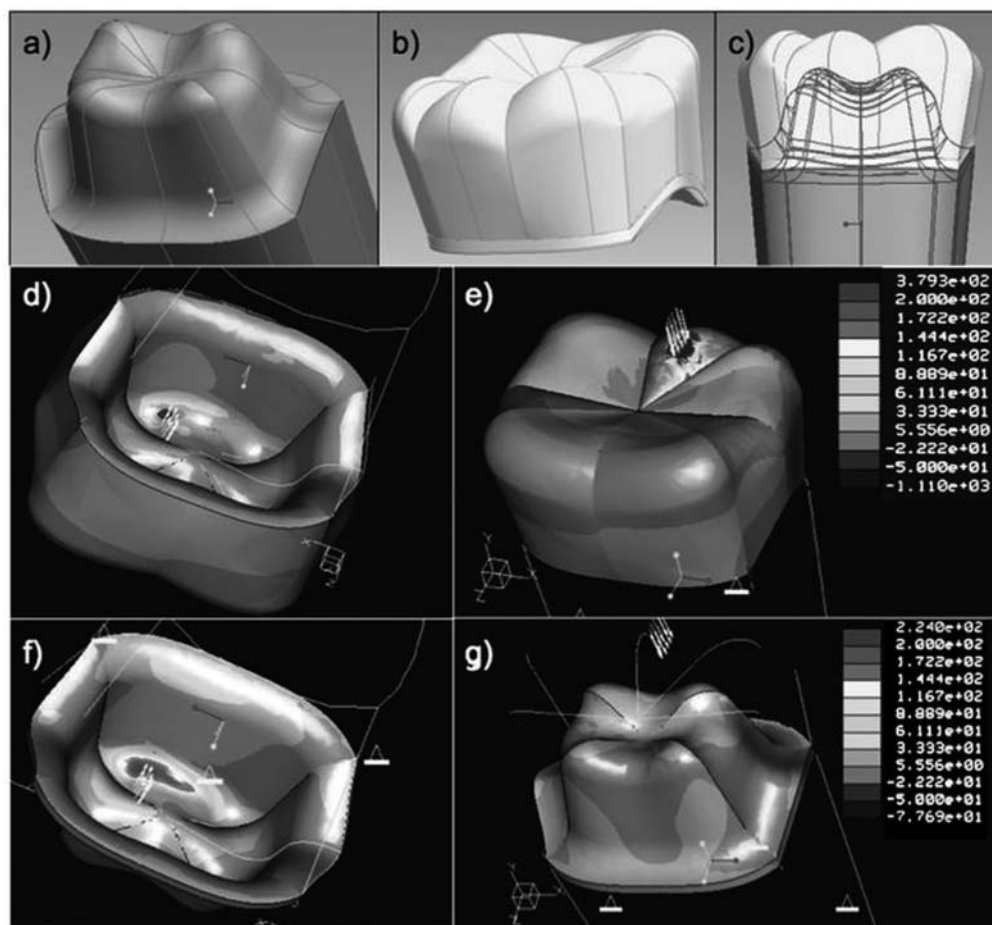


**Figure 1.** Finite element analysis results. **(A)** CAD-designed four-cusp right first molar preparation and **(B)** cement, zirconia core, and veneer solid models. **(C)** Assembled preparation, cement, zirconia core, and veneer solid models. **(D,E)** Resulting maximum principal stress obtained on the veneer solid under a 1200-N vertical load applied on the mesial-distal cusp of the veneer solid; and **(F,G)** resulting maximum principal stress obtained on the zirconia core solid under a 1200-N vertical load applied on the mesial-distal cusp of the veneer solid. Note the high maximum principal stress values observed in the bottom part of the zirconia core layer **(F)** at the region immediately below the load, and at the cervical region.

cusp ridge on the veneer layer. Both uni-axial and bi-axial loading was investigated, and regions of maximum principal stress were determined.

### Specimen Fabrication

Seventeen anatomically correct crowns were fabricated based on the design used in the finite element analysis described above. The CAD file of the prepared tooth was converted to *.igs files, imported into a milling machine, and plastic models were generated (Fig. 2a). The plastic models were placed in a dental articulator (Fig. 2b) with opposing and adjacent dentition. Impressions of the prepared, adjacent, and opposing teeth were taken (Aquasil, Dentsply, York, PA, USA) and sent to a CAD/CAM milling center (3M/ESPE, St. Paul, MN, USA), where 0.5-mm-thick zirconia cores (LAVA, 3M/ESPE) were fabricated. These cores were veneered with porcelain (LAVA Veneer, 3M/ESPE by a commercial dental laboratory (Marotta Dental Studio, Huntington, NY, USA), creating crowns with clinically appropriate fit and geometry (Fig. 2c).
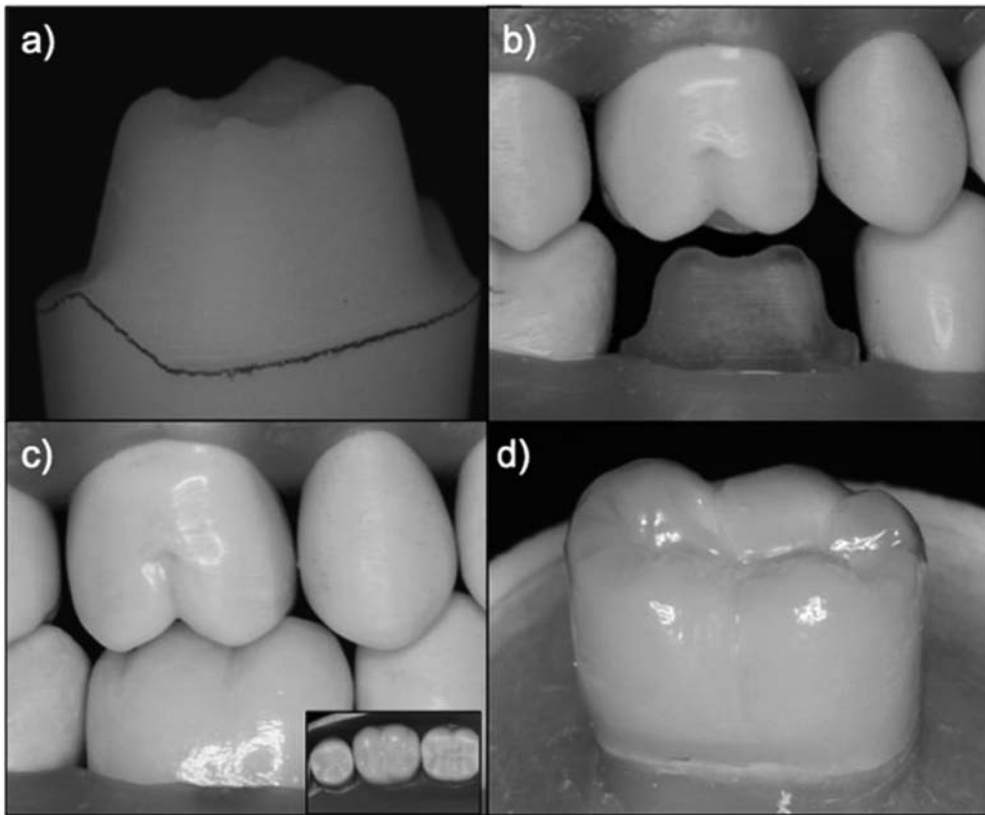
**Figure 2.** Crowns made from the anatomically correct crown model. **(A)** Plastic prototype of the prepared tooth, **(B)** plastic prototype inserted into a dental arch and articulator, **(C)** all-ceramic crown with 0.5-mm zirconia core **(D)** crown cemented onto plastic prototype, embedded in acrylic resin in preparation for load testing.

through a 6.25-mm-radius tungsten carbide (WC) indenter on the lingual aspect of the disto-facial cusp at a rate of 1 mm/min. The mean single load-to-fracture value was used to establish profiles for step-stress fatigue tests.

For sliding-contact mouth-motion step-stress fatigue, the specimens were attached to a servo-all-electric system (800L, TestResources, Shakopee, MN, USA), and subjected under water to 1 of 3 step-stress profiles following the distribution 4:2:1 (light, moderate, and aggressive profiles, respectively, based upon the single load-to-fracture mean value) and tested until failure or survival (Nelson, 1990).

All mechanical testing was performed with a WC indenter of 6.25 mm diameter sliding 0.7 mm lingually down the disto-facial cusp, beginning at 0.5 mm lingual to the cusp tip, simulating aspects of natural occlusion. A Weibull curve and reliability for completion of a mission of 50,000 cycles at 300-N load were calculated (Zhao and Elsayed, 2005) (Alta Pro7, Reliasoft, Tucson, AZ, USA).

Using polarized light microscope (MZ-APO, Carl Zeiss MicroImaging, Thornwood, NY, USA) and SEM (Model 3500S, Hitachi, Osaka, Japan) imaging, we evaluated crowns and fracture segments (SEM). Fracture modes were compared with regions of high MPS observed in the FEA model, as well as reported clinical failure modes (Raigrodski *et al.*, 2006; Sailer *et al.,* 2007; Tsalouchou *et al.*, 2008).

In parallel, 17 prepared tooth replicas were fabricated from high-modulus polyvinylsiloxane impressions (Aquasil, Dentsply) of the machined plastic models. The impressions were filled with layers of resin-based composite (Z100, 3M/ESPE) and cured according to the manufacturer's recommendations. The replicas were stored in distilled water at 37°C for at least 30 days to ensure hydration and eliminate any effects of water-uptake dimensional expansion after crown cementation (Huang *et al.*, 2007).

At cementation, a layer of metal primer (Alloy Primer, Kuraray, Ltd, Osaka, Japan) was applied to the internal surface of the zirconia core (no sandblasting was used). The crowns were then cemented (RelyX Unicem, 3M/ESPE) under a 10-N load onto the tooth replica.

The crown-tooth replica was embedded in acrylic resin (Orthoresin, Degudent, Mainz, Germany) in a 1-inch-diameter PVC tube. The crown buccal margin was placed 2 mm above the surface of the resin, with the long axis of the crown-tooth replica and tube aligned (Fig. 2d). Specimens were stored in water.

## Single Load to Fracture and Sliding-contact Mouth-motion Step-stress Fatigue

One week after cementation, 3 crowns were subjected to single load-to-fracture. Sliding-contact stress fatigue was then performed on the remaining crowns (n = 14). For single load-to-fracture, the specimens were mounted in a universal testing machine (Model 5566, Instron, Acton, MA, USA), and load-to-fracture was applied

## RESULTS

### Finite Element Analysis

Variations in maximum principal stress developed on the crown veneer and zirconia core solids (Figs. 2d-2g). High stress levels were observed directly below the load region for both veneer and zirconia core solids (Figs. 2d-2g), and higher stress levels were observed at the zirconia core region in contact with the cement layer. Increased levels of stress concentration were also observed at the margin regions of the zirconia core, including proximal regions (Figs. 2f, 2g).

### Single Load-to-Fracture and Sliding-contact Mouth-motion Step-stress Fatigue

The single load-to-fracture mean value was $1227 \pm 221$ N (utilized as the rationale for the 1100-N load condition on the FEA model). The
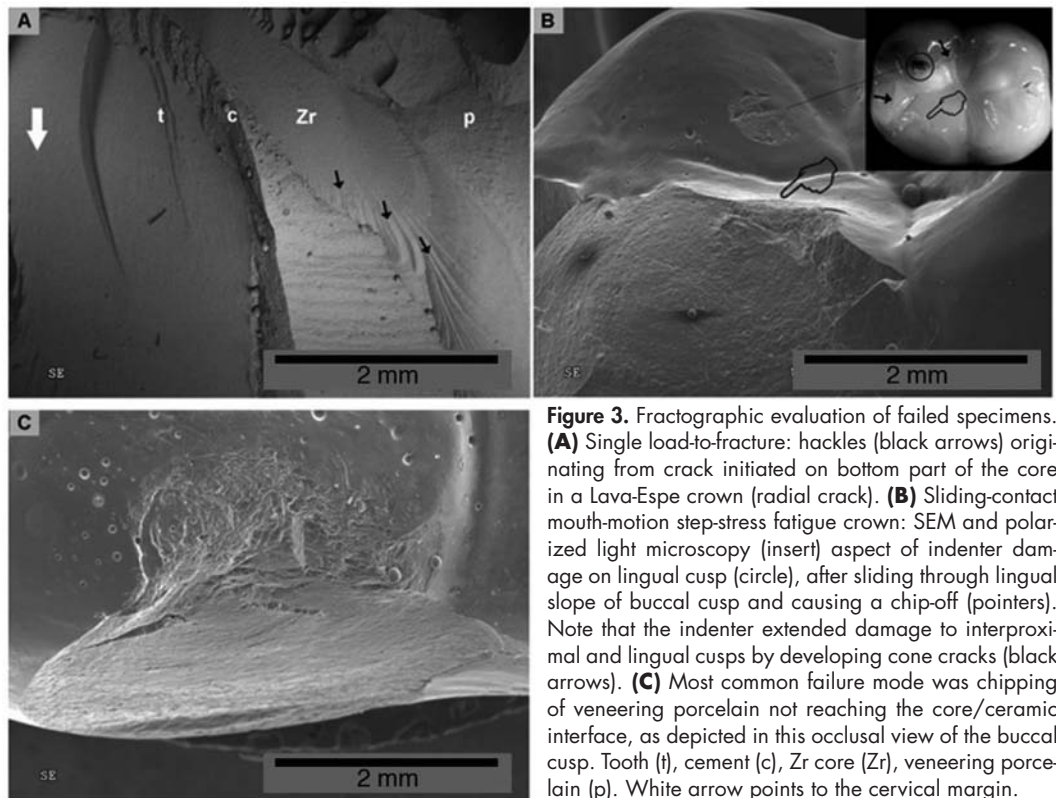
failure mode observed for all but one single load-to-fracture specimen showed a radial crack propagating from the zirconia core region in contact with the cement surface (Fig. 3a), resulting in a catastrophic failure fracture mode, including both the veneer and zirconia core (Fig. 3a). The fracture extended from the cusp ridge all the way through the zirconia cervical margin and cement layer. One single load-to-fracture specimen exhibited a cohesive veneer fracture similar to those observed in sliding-contact mouth-motion step-stress fatigue (Figs. 3b, 3c). Based the mean single load-to-fracture, the maximum load for sliding-contact mouth-motion step-stress fatigue profiles was set at 600 N.



**Figure 3.** Fractographic evaluation of failed specimens. **(A)** Single load-to-fracture: hackles (black arrows) originating from crack initiated on bottom part of the core in a Lava-Espe crown (radial crack). **(B)** Sliding-contact mouth-motion step-stress fatigue crown: SEM and polarized light microscopy (insert) aspect of indenter damage on lingual cusp (circle), after sliding through lingual slope of buccal cusp and causing a chip-off (pointers). Note that the indenter extended damage to interproximal and lingual cusps by developing cone cracks (black arrows). **(C)** Most common failure mode was chipping of veneering porcelain not reaching the core/ceramic interface, as depicted in this occlusal view of the buccal cusp. Tooth (t), cement (c), Zr core (Zr), veneering porcelain (p). White arrow points to the cervical margin.

In total, 14 crowns were utilized for the sliding-contact mouth-motion step-stress fatigue testing: 8 specimens on Profile 1, 4 on Profile 2, and 2 on Profile 3. All 14 specimens failed cohesively within the veneer layer (Fig. 3). This cohesive fracture originated in regions directly below the indenter sliding path (Figs. 3b, 3c). In only one specimen did the fatigue fracture extend to include the veneer-core interface.

The observed step-stress-derived probability Weibull plot at a 200-N load resulted in a Weibull modulus of 1.7 (Fig. 4), which indicated that fatigue was not a strong acceleration factor and that failures would be distributed over a wide range of load cycles. Step-stress-accelerated fatigue studies facilitate estimates of reliability at a given load level. The calculated crown reliability with 90% confidence bounds for a 200-N load and a mission of 50,000 cycles was equal to 0.48 (0.68 - 0.25). This indicates that the cumulative damage from loads reaching 200 N would lead to veneer failure in over 50% of the specimens tested by 50,000 cycles

## DISCUSSION

Different failure modes were expressed in single load-to-fracture and sliding-contact mouth-motion step-stress fatigue, with the latter more closely approximating failures being reported clinically. The discrepancy between clinically observed failure modes and laboratory *in vitro* testing has been noted for some time (Kelly, 1999). Usually, single load-to-failure tests and mouth-motion fatigue of simplified geometries (flat layers or crown-like structures) (Rekow and Thompson, 2007) in laboratory settings have provided limited data to guide the development of all-ceramic systems, necessitating time-consuming clinical trials before a basic understanding of the varied biomechanical behavior of all-ceramic systems becomes evident. The present study is

the first to include an anatomically correct standardized computer design to generate laboratory specimens allowing for evaluation by computer mechanical simulation of single load-to-fracture failure and mouth-motion (contact-slide-lift-off) fatigue.

Given the known highly accelerated failure from surface cracks with mouth-motion sliding contacts in water (JW Kim *et al.*, 2007), our 100% failure within the veneers can be anticipated. Sliding contact fatigue in water appears critical for simulation of occlusal conditions.

The finite element analysis output for the zirconia core-veneer system under a load of 1200 N (near the average force observed in single load-to-fracture) showed high stress concentrations in both veneer and zirconia core solids. This is in agreement with the site of crack initiation of the single load-to-fracture crowns that failed through the zirconia core, but not with those tested in fatigue, which failed cohesively in the veneer layer (clinically observed critical failure mode) (Sailer *et al.*, 2007).

The sliding-contact mouth-motion step-stress fatigue testing in water configuration used translation of the indenter 0.5-0.7 mm along the crown surface from the disto-facial cusp tip down the cusp ridge toward the central fossa. Indenter translation simulates approximating tooth surfaces during mastication. Such translation has been shown to be highly deleterious, due to stress field extension and magnification by water in partial cone cracks (B Kim *et al.*, 2007; JW Kim *et al.*, 2007). The cohesive failure found beneath the indenter path suggests that this hydraulically assisted damage mode was operational in these anatomical crowns. The high hardness of the tungsten carbide indenter compared with that of glass or enamel only slightly changed the rate of crack initiation and evolution for the veneering porcelain (Bhowmick *et al.*, 2007a).

All sliding-contact mouth-motion step-stress fatigue specimens failed through the veneer layer from cone crack propagation.
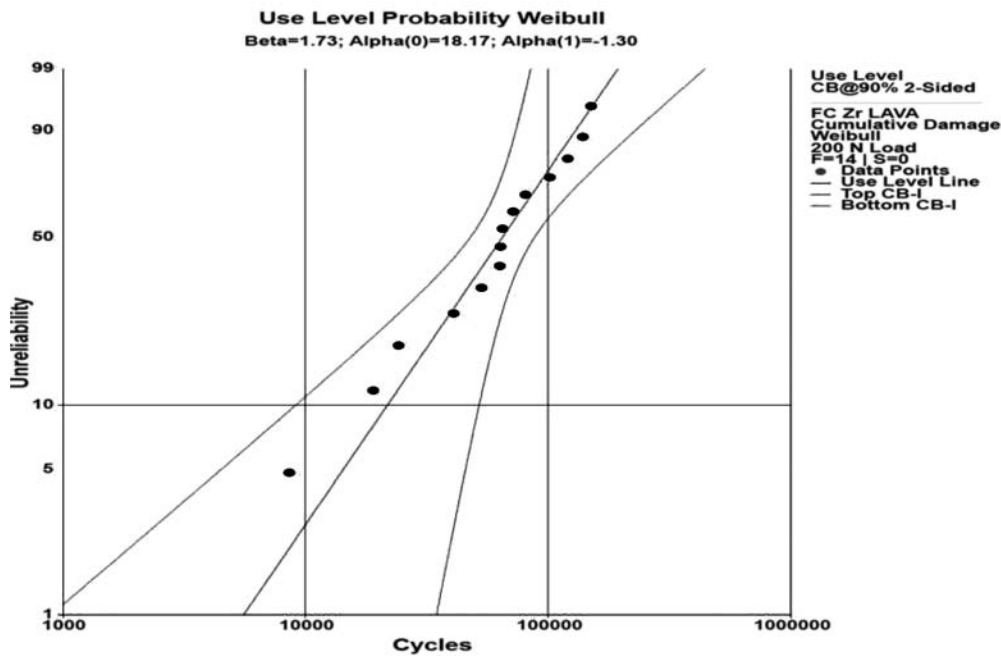
**Figure 4.** Weibull distribution graph for the Lava all-ceramic crowns depicts unreliability *vs.* number of cycles (90% two-sided confidence bounds) with a load of 200 N. Weibull modulus of 1.7 indicates that fatigue was not a strong accelerator of failure.

Clinical observations have shown that veneer failures on metal and all-ceramic cores are the dominant failure mode in single crowns and bridges (Raigrodski *et al.*, 2006; Pjetursson *et al.*, 2007; Sailer *et al.*, 2007). The fatigue wake hackle lines observed in the SEM (not shown here) indicate that failure progressed from the contact area through the body of the porcelain, as noted in clinical replicas (Scherrer *et al.*, 2008), suggesting that the methodology used was successful in simulating clinical scenarios. As hypothesized, the mouth-motion sliding-contact fatigue resulted in veneer chipping, reproducing clinical findings allowing for investigations into the underlying causes of such failures.

Based upon these findings, sliding-contact fatigue testing in water of clinically relevant crown geometry is recommended to simulate clinical conditions. The reliability established for the veneer-core system used provides the basis for comparison between materials and changes in processing conditions prior to further mechanical testing. Changing processing conditions appears to be critical to the veneered zirconia, since large chipping not exposing the veneer indicates residual stress states in the porcelain above the interface with the zirconia. This may be attributed to the very low thermal diffusivity of zirconia compared with that of alumina and metals (Rekow and Thompson, 2007). We suggest that the test methodology used herein could accelerate understanding of the relationships between materials and clinical success, as well as serving as a platform for the development of future all-ceramic crown systems.

## ACNOWLEDGMENTS

## REFERENCES

Bhowmick S, Melendez-Martinez JJ, Hermann I, Zhang Y, Lawn BR (2007a). Role of indenter material and size in veneer failure of brittle layer structures. *J Biomed Mater Res B Appl Biomater* 82:253-259.

Bhowmick S, Melendez-Martinez JJ, Zhang Y, Lawn BR (2007b). Design maps for failure of all-ceramic layer structures in concentrated cyclic loading. *Acta Materialia* 55:2479-2488.

Deng Y, Lawn BR, Lloyd IK (2002). Characterization of damage modes in dental ceramic bilayer structures. *J Biomed Mater Res* 63:137-145.

Huang M, Thompson VP, Rekow ED, Soboyejo WO (2007). Modeling of water absorption induced cracks in resin-based composite supported ceramic layer structures. *J Biomed Mater Res B Appl Biomater* 84:124-130.

Kelly JR (1999). Clinically relevant approach to failure testing of all-ceramic restorations. *J Prosthet Dent* 81:652-661.

Kim B, Zhang Y, Pines M, Thompson VP (2007). Fracture of porcelain-veneered structures in fatigue. *J Dent Res* 86:142-146.

Kim JW, Kim JH, Thompson V, Zhang Y (2007). Sliding contact damage in layered ceramic structures. *J Dent Res* 86:1046-1050.

Kohal RJ, Klaus G (2004). A zirconia implant-crown system: a case report. *Int J Periodont Rest Dent* 24:147-153.

Kohal RJ, Klaus G, Strub JR (2006). Zirconia-implant-supported all-ceramic crowns withstand long-term load: a pilot investigation. *Clin Oral Implants Res* 17:565-571.

Manicone PF, Rossi Iommetti P, Raffaelli L (2007). An overview of zirconia ceramics: basic properties and clinical applications. *J Dent* 35:819-826.

Nelson W (1990). Model and data analysis for step and varying stress. In: Accelerated testing: statistical models, test plans, and data analysis. New York: John Wiley & Sons, pp. 493-520.

Pjetursson BE, Sailer I, Zwahlen M, Hammerle CH (2007). A systematic review of the survival and complication rates of all-ceramic and metal-ceramic reconstructions after an observation period of at least 3 years. Part I: single crowns. *Clin Oral Impl Res* 18(Suppl 3):73-85; *erratum* in *Clin Oral Impl Res* 19:326-328, 2008.

Raigrodski AJ, Chiche GJ, Potiket N, Hochstedler JL, Mohamed SE, Billiot S, *et al.* (2006). The efficacy of posterior three-unit zirconium-oxide-based ceramic fixed partial dental prostheses: a prospective clinical pilot study. *J Prosthet Dent* 96:237-244.

Rekow D, Thompson VP (2007). Engineering long term clinical success of advanced ceramic prostheses. *J Mater Sci Mater Med* 18:47-56.

Sailer I, Feher A, Filser F, Gauckler LJ, Luthy H, Hammerle CH (2007). Five-year clinical results of zirconia frameworks for posterior fixed partial dentures. *Int J Prosthodont* 20:383-388.

Scherrer SS, Quinn GD, Quinn JB (2008). Fractographic failure analysis of a Procera AllCeram crown using stereo and scanning electron microscopy. *Dent Mater* 24:1107-1113.

Tsalouchou E, Cattell MJ, Knowles JC, Pittayachawan P, McDonald A (2008). Fatigue and fracture properties of yttria partially stabilized zirconia crown systems. *Dent Mater* 24:308-318.

Zahran M, El-Mowafy O, Tam L, Watson PA, Finer Y (2008). Fracture strength and fatigue resistance of all-ceramic molar crowns manufactured with CAD/CAM technology. *J Prosthodont* 17:370-377.

Zhao W, Elsayed AE (2005). A general accelerated life model for step-stress testing. *IEEE Transactions* 37:1059-1069.